2010

# Magnetic antiphase domains in Co/Ru/Co trilayers

Zhen Li
*University of Nebraska - Lincoln*

Ralph Skomski
*University of Nebraska at Lincoln*, rskomski2@unl.edu

Steven A. Michalski
*University of Nebraska-Lincoln*, smichalski2@unl.edu

Lanping Yue
*University of Nebraska-Lincoln*, lyue2@unl.edu

Roger D. Kirby
*University of Nebraska-Lincoln*, rkirby1@unl.edu

# Magnetic antiphase domains in Co/Ru/Co trilayers

Zhen Li,[1,a)] Ralph Skomski,[1,2] Steven Michalski,[1,2] Lanping Yue,[2] and Roger D. Kirby[1,2]
[1]*Department of Physics and Astronomy, University of Nebraska, Lincoln, Nebraska 68588, USA*
[2]*Nebraska Center for Materials and Nanoscience, University of Nebraska, Lincoln, Nebraska 68588, USA*

(Presented 19 January 2010; received 31 October 2009; accepted 16 December 2009; published online 21 April 2010)

Ultrathin Co/Ru/Co trilayers are investigated experimentally by magnetization curves and magnetic-force microscopy (MFM). Emphasis is on the domain-wall fine structure of antiphase domain walls in the films. The trilayers are produced by sputtering and consist of two Co layers of equal thickness (5 nm), exchange-coupled through a Ru layer of variable thickness. The sign and magnitude of the interlayer exchange are tuned by the thickness of the Ru interlayer. The exchange and its distribution are investigated by measurements of the static magnetization curves. For a Ru thickness of 0.4 nm, the exchange is predominantly antiferromagnetic and the MFM images show fairly immobile domain walls. Micromagnetic model calculations yield immobile antiphase domain walls whose thickness decreases with increasing magnetic field but is typically of the order of 100 nm in agreement with experiment. © *2010 American Institute of Physics*. [doi:10.1063/1.3367966]

## I. INTRODUCTION

Since the discovery of magnetic domains by von Hámos and Thiessen[1] and Bitter[2] and their theoretical explanation,[3,4] magnetic domains and domain walls have been a fascinating and technologically important research subject.[5] Our focus is on ultrathin Co/Ru/Co trilayers. Thin films composed of magnetic layers separated by a nonmagnetic spacer have received considerable attention in recent years because they are used in spin-valve devices.[6] However, the spin-electronics applications are not the only aspect of these structures and there are interesting domain phenomena. Rührig *et al.*[7] observed a domain transition from ripple to patch pattern in Fe/Cr/Fe layered structures. A key factor in the understanding is the interlayer exchange coupling through the spacer layer. The interlayer coupling $J$ generally oscillates as function of the layer thickness,[8] and these oscillations between ferromagnetism (FM) and anti-FM (AFM) are basically due to the Ruderman–Kittel–Kasuya–Yosida interaction mediated by the conduction electrons of the spacer layer.[9,10]

Heavy transition metals (4d and 5d series) have attracted considerable attention as spacer layers in electronics, and this includes the 4d element ruthenium, which can be used to realize a robust antiferromagnetic coupling between ferromagnetic layers. Gornakov *et al.*[11] studied the magnetization reversal in coupled Co/Ru/Co trilayers where the bottom layer acts as a pinning layer. Zhang *et al.*[12] investigated the exchange coupling of Co/Ru/Co trilayers using ferromagnetic resonance. Gubbiotti *et al.*[13] and Li *et al.*[14] discussed asymmetric Co/Ru/Co films as a function of the ferromagnetic layer thickness. Our present paper focuses on magnetic domains in Ru-containing trilayers without in-plane anisotropy and top and bottom layers of equal thickness.

## II. EXPERIMENT

A series of trilayer Co/Ru/Co thin films were produced by magnetron sputtering with a base pressure of approximately $1\times10^{-7}$ Torr on silicon substrates. The thicknesses of the top and bottom Co layers were fixed at 5 nm, while the thickness of Ru interlayer was varied from 0 to 1 nm with steps of 0.1 nm. The in-plane $M(H)$ magnetization curves were measured using a MicroMag Model 2900 alternating gradient-force magnetometer. To perform the room temperature MFM imaging, we used a DI Dimension 3100 SPM in tapping/lift mode with a magnetic field applied in the film plane.

## III. RESULTS AND DISCUSSION

Figure 1 shows the $M(H)$ magnetization curves for different Ru thicknesses; both the magnetic field and the measured magnetization are in the film plane. We also checked the magnetization in different in-plane directions and found no evidence of in-plane magnetic anisotropy, in contrast to the strong uniaxial Co anisotropy induced by oblique sputtering of a Ta underlayer in a related system.[15] With increasing Ru thickness, the reduced remanence $M(0)/M_s$ decreases from nearly 1 to nearly 0. The interpretation of the $M(H)$

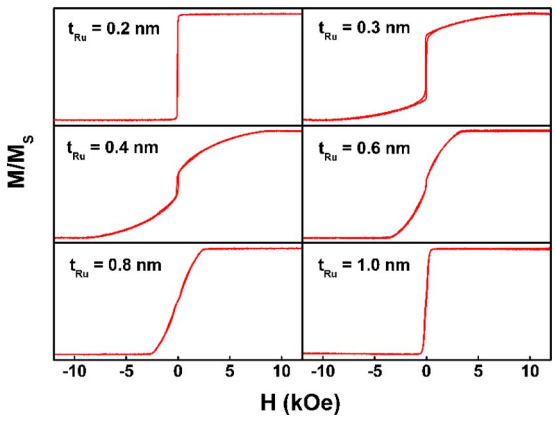


FIG. 1. (Color online) Room-temperature magnetization curves for different Ru thicknesses. The magnetic field is in the sample plane.

[a)]Electronic mail: zhen.li@huskers.unl.edu.

 

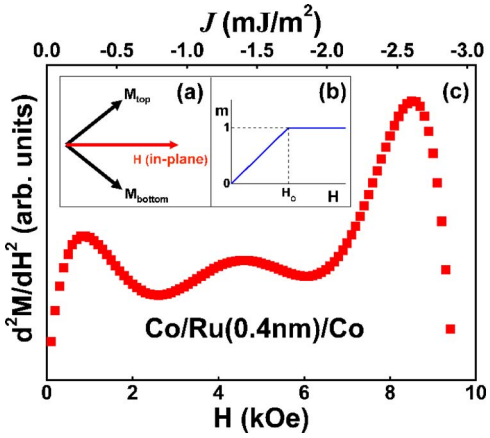


FIG. 2. (Color online) (a) AFM configuration with in-plane field applied and (b) its corresponding $M(H)$ curve; and (c) lateral distribution of exchange constant derived from the experimental $M(H)$ curve.

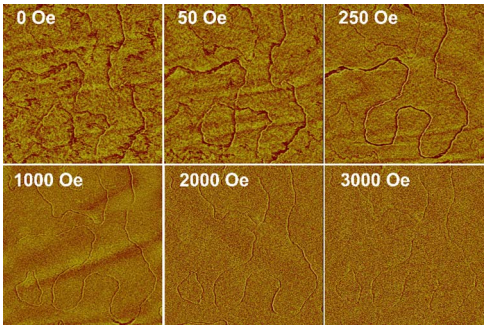


FIG. 3. (Color online) MFM picture of the domain structure of 0.4 nm Ru trilayer square of size $15\times15$ $\mu m^2$. The magnetic field is in the film plane.

curves are discussed below. To model the trilayers, it is convenient to introduce the reduced magnetization $\mathbf{m}=\mathbf{M}/M_s$ and to start from the energy per unit area

$$E = At[(\nabla\cdot\mathbf{m_t})^2+(\nabla\cdot\mathbf{m_b})^2]-J\mathbf{m_t}\cdot\mathbf{m_b}+\frac{\mu_o}{2}M_s{}^2t(m_{z,t}{}^2 + m_{z,b}{}^2)-\mu_oM_stH\cdot(\mathbf{m_t}+\mathbf{m_b}). \quad (1)$$

Here $A$ is the exchange stiffness of Co (about 20 pJ/m), $t$ is the thickness of one Co layer, and the indices t and b stand for the top and bottom Co layers, respectively. The measured Co magnetization was 1225 kA/m, and no magnetocrystalline anisotropy was detected.

For the in-plane static magnetization measurements, we then take in account that $m_{z,t}=m_{z,b}=0$ and make the reasonable assumption that the magnetization is homogeneous $\nabla\mathbf{m_t}=\nabla\mathbf{m_b}=0$. Equation (1) therefore reduces to

$$E=-J\mathbf{m_t}\cdot\mathbf{m_b}-\mu_oM_stH\cdot(\mathbf{m_t}+\mathbf{m_b}). \quad (2)$$

The behavior of this equation depends on whether the coupling is FM ($J>0$) or AFM ($J<0$). Moreover, due to lateral thickness variations, we expect a certain distribution $P(J)$ of the exchange coupling. In the FM case, the $M(H)$ consists of a single big step at $H=0$, irrespective of the magnitude or distribution of $J$. This step is clearly visible in Fig. 1, especially for thin Ru layers. Physically, the net magnetization is always parallel to the external field.

The AFM configuration, illustrated in Fig. 2(a), is well known to correspond to an $M(H)$ curve of constant slope[16] until saturation is reached at $H_o=-2J/(tM_s)$ [Fig. 2(b)]. The field $H_o$ at which the magnetization saturates depends on $J$ so that a distribution $P(J)$ of AFM exchange constants smears the singularity at $H_o$. This smearing is seen in the loops of Fig. 1, especially for thicknesses from 0.3 to 0.8 nm, but there is also a FM contribution. The coexistence of FM and AFM couplings is consistent with the observation that a Ru layer can induce the parallel or antiparallel spin orientations in adjacent ferromagnetic layers.[17,18] In our films, the FM contribution decreases with increasing Ru thickness.

To determine the antiferromagnetic part of $P(J)$, we exploit that the second derivative of the function shown in Fig. 2(b) is essentially a delta function, $\delta(H\text{-}H_o)$. Aside from a normalization factor, $P(J)$ is therefore equal to $d^2m/dH^2$ measured at $H=-2J/(tM_s)$. This makes it possible to extract the AFM part of the distribution from the $M(H)$ curves. The curved part of the loops could be well fit with a seventh order polynomial and the resulting curve was differentiated to obtain the result in Fig. 2(c) for $t_{Ru}=0.4$ nm sample. The distribution is peaked, probably as a consequence of the discrete Ru layer thickness, and exhibits a pronounced maximum around $J=-2.6$ mJ/m$^2$. On the other hand, the interlayer exchange coupling can also be investigated by dynamical methods which we will publish elsewhere. The simulation of the dynamical data yields a similar value of $J$ ($-2.1$ mJ/m$^2$ for $t_{Ru}=0.4$ nm sample).

Figure 3 shows MFM images for 0.4 nm Ru in low and moderate magnetic fields applied in the film plane. The domains are separated by meandering domain walls. A striking feature, related to the predominantly antiferromagnetic character of the exchange, is the immobility of the domain walls in a magnetic field. We also notice that the domain walls get narrower as the field increases, from about $\delta_w=350$ nm for low fields to about 100 nm. To calculate the domain-wall width, we start from Eq. (1) and take into account that the magnetostatic term vanishes for in-plane magnetizations. Since $\delta_w \gg t$, magnetic charges inside the film can also be neglected.

It is convenient to write the in-plane angles of the Co-layer magnetization as $\theta_t=\pi/2-\phi-\chi$ and $\theta_b=\pi/2+\phi-\chi$, where the total magnetization along the magnetic field direction is $M_s[\cos(\theta_t)+\cos(\theta_b)]$ and $\phi$ and $\lambda$ vary as a function of the distance from the center of the wall. The procedure amounts to separately considering the net magnetization (angle $\phi$) and the deviation $\lambda$ from ideal antiparallel alignment. Figure 4 illustrates the corresponding domain-wall fine structure. This transformation reduces Eq. (1) to

$$E=2At[(\nabla\phi)^2+(\nabla\chi)^2]+J\cos(2\chi)-2\mu_oM_stH\cos\phi\sin\chi. \quad (3)$$

The (negative) exchange suppresses the spin misalignment so that $\lambda\sim0$ in small fields. The next step is to neglect $(\nabla\chi)^2\ll(\nabla\phi)^2$ and to minimize $E$ with respect to the small quantity $\chi$. This yields

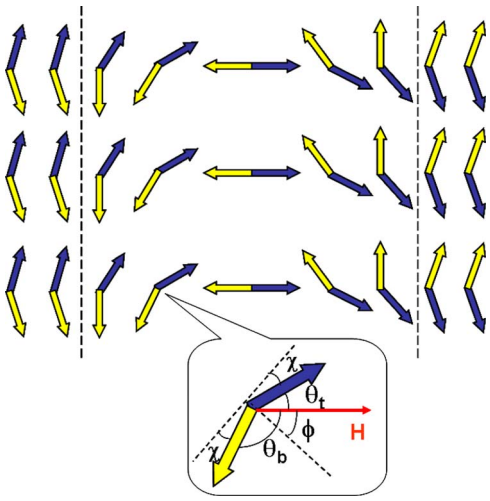


FIG. 4. (Color online) Domain-wall fine structure of the trilayer. The angles $\theta_t$, $\theta_b$, $\phi$, and $\chi$ are defined for each point in the film plane, and the spin structure is obtained by minimizing the corresponding energy functional.

$$\sin(\chi) = -\frac{\mu_o M_s t H}{2J}\cos\,\phi, \tag{4}$$

and, after substitution into Eq. (4)

$$E = 2At(\nabla\phi)^2 + \frac{(\mu_o M_s t H)^2}{2J}\cos^2\,\phi + J. \tag{5}$$

This energy has the functional structure of an ordinary Bloch-wall energy[5,19] with the domain-wall width

$$\delta_w = 2\pi\frac{\sqrt{-AJ/t}}{\mu_o M_s H}. \tag{6}$$

This equation explains the decrease of the domain-wall width with increasing magnetic field and predicts the correct order of magnitude $\delta_w \sim 100$ nm.

Our experiments and model calculations provide a fairly comprehensive picture of the interactions and magnetization processes in the Co/Ru/Co trilayers. The remaining discrepancies probably reflect contributions such as biquadratic exchange due to interface roughness and fluctuations of the Co layer thicknesses. However, these corrections do not affect the basic picture.

A striking feature of the domains in Fig. 3 is that an external field does not change the domain-wall positions. By contrast, ferromagnetic domains in soft-magnetic materials move very easily when subjected to an external magnetic field, unless they are captured by a pinning site (structural defect). The present system does not exhibit any substantial pinning, and each hysteresis-loop cycle seems to randomly create a new domain-wall configuration. The reason for this difference is the dependence of the Zeeman energy on the domain-wall position. Domain-wall motion in ferromagnets reduces the Zeeman energy by enhancing the volume fraction of parallel domains at the expense of antiparallel domains. In the present system, the Zeeman energy is independent of the domain-wall position. Figure 4 shows that the Zeeman energy is somewhat reduced in the center of the wall, but the adjacent regions on the left-and right-hand sides of the wall have the same Zeeman energy density. This means that any shift of the wall to the left or right leaves the Zeeman energy unchanged, and there is no net force acting on the wall. Compared to the AFM exchange in typical bulk antiferromagnets, the interlayer exchange field per involved atom is relatively small and comparable to typical laboratory-scale magnetic fields. This leads to relatively largely tilting angles $\chi$ [Eq. (4)] and means that the effect is easily detected by MFM.

## IV. CONCLUSIONS

In conclusion, our Co/Ru/Co trilayers exhibit a mixture of FM and AFM exchange constants caused by lateral variations in the Ru thickness, and the exchange constants have been analyzed with the help of magnetization curves. The ratio of FM to AFM contributions decreases as the Ru thickness increases from 0.2 to 1 nm, and explicit distribution functions have been obtained for the AFM part of the distribution. For in-plane magnetic fields, the films exhibit antiphase domains separated by immobile domain walls. We have calculated the fine structure and width of these domains walls, and our calculations explain why the domain-wall thickness decreases from about 350 nm in low fields to about 100 nm in moderate fields.

## ACKNOWLEDGMENTS

This work has been supported by NSF-MRSEC (Grant No, DMR-0820521) and NCMN. The authors are grateful to D. J. Sellmyer for stimulating discussions.

[1] L. V. Hámos and P. A. Thiessen, Z. Phys. **71**, 442 (1931).
[2] F. Bitter, Phys. Rev. **38**, 1903 (1931).
[3] F. Bloch, Z. Phys. **74**, 295 (1932).
[4] L. Landau and E. Lifshitz, Phys. Z. Sowjetunion **8**, 153 (1935).
[5] A. Hubert and R. Schäfer, *Magnetic Domains* (Springer-Verlag, Berlin, 1998).
[6] Z. Zhao, P. Mani, G. J. Mankey, G. Gubbiotti, S. Tacchi, F. Spizzo, W. T. Lee, C. T. Yu, and M. J. Pechan, Phys. Rev. B **71**, 104417 (2005).
[7] M. Rührig, R. Schäfer, A. Hubert, R. Mosler, J. A. Wolf, S. Demokritov, and P. Grünberg, Phys. Status Solidi A **125**, 635 (1991).
[8] S. S. P. Parkin, N. More, and K. P. Roche, Phys. Rev. Lett. **64**, 2304 (1990).
[9] R. Coehoorn, Phys. Rev. B **44**, 9331 (1991).
[10] P. Bruno and C. Chappert, Phys. Rev. Lett. **67**, 1602 (1991).
[11] V. S. Gornakov, V. I. Nikitenko, W. F. Egelhoff, Jr., R. D. McMichael, A. J. Shapiro, and R. D. Shull, J. Appl. Phys. **91**, 8272 (2002).
[12] Z. Zhang, L. Zhou, P. E. Wigen, and K. Ounadjela, Phys. Rev. B **50**, 6094 (1994).
[13] G. Gubbiotti, S. Tacchi, G. Carlotti, G. Socino, F. Spizzo, Z. Zhao, P. Mani, and G. J. Mankey, J. Magn. Magn. Mater. **286**, 468 (2005).
[14] H. Y. Li, S. M. Zhou, J. Du, and A. Hu, Phys. Status Solidi **191**, 583 (2002).
[15] R. D. McMichael, C. G. Lee, J. E. Bonevich, P. J. Chen, W. Miller, and W. F. Egelhoff, Jr., J. Appl. Phys. **88**, 5296 (2000).
[16] J. S. Smart, *Effective Field Theories of Magnetism* (Saunders, Philadelphia, 1966).
[17] P. J. H. Bloemen, H. W. Van Kesteren, H. J. M. Swagten, and W. J. M. de Jonge, Phys. Rev. B **50**, 13505 (1994).
[18] R. Schäfer, A. Hubert, and S. S. P. Parkin, IEEE Trans. Magn. **29**, 2738 (1993).
[19] R. Skomski, *Simple Models of Magnetism* (University Press, Oxford, 2008).